Seismic Evaluation of Beam-Column Joints in Older Concrete Exterior Frames

Dawn Lehman[1], John Stanton[2], and Daniel Alire[3]

ABSTRACT

This paper describes an experimental study on beam-column joints in older reinforced concrete exterior frames subjected to seismic loading. Because joints in pre-1970s construction were not designed using modern seismic design guidelines, they typically contain no transverse reinforcement and may be subjected to a wide range of levels of joint shear stress demand. In current codes and recommendations for seismic design and evaluation, simple expressions are used typically to design the joint, and a strut-mechanism approach has been adopted to assess the strength. However, prior and ongoing research has shown that joint behavior is more complicated than implied by these documents and that defining failure by static strength alone is not sufficient to describe performance.

A previous experimental research study, conducted by the principal investigators, has demonstrated that the joint response depends on several parameters, including the demand history. To investigate in greater detail the influence of the joint shear stress demand on the response, the research study described herein was conducted. The data from the two programs were then combined to establish probabilistic relationships between joint damage and

[1] Department of Civil and Environmental Engineering, University of Washington, Seattle WA

[2] Department of Civil and Environmental Engineering, University of Washington, Seattle WA

[3] KPFF Consulting Engineers, Seattle WA

Engineering Demand Parameters, such as shear stress and strain, and to obtain estimates of joint stiffness for use in the seismic analysis of older structures.

Subject Headings: Seismic Evaluation, Beam-Column Joints, Reinforced Concrete Frames, Performance-Based Design

INTRODUCTION

Significant shear forces develop in the joints of reinforced concrete moment frames that are subjected to seismic loading. In frames built before the mid-1970s, the joints typically contain no transverse reinforcement, so the shear resistance must be developed by the concrete alone. The joint shear demands also vary considerably from one structure to another. Contemporary joints contain transverse reinforcement and experience joint shear stress demands that are limited by code requirements, but they are still susceptible to seismic damage. It is therefore logical to expect the joints in older frames to be even more vulnerable (Mosier 2000).

Most previous studies have concentrated on joints that contain transverse reinforcement, with the objective of improving joint response. However, a large number of older reinforced concrete frames exist and these frames lack joint reinforcement. Limited research has been conducted on such joints, and data are needed to support the development and refinement of guidelines for evaluating them.

ASCE-41 (2007), which is based on FEMA 356 (2000), provides a model for predicting the joint shear response, but Walker (2001) demonstrated its shortcomings. The first of these is that it conservatively predicts strength which will result in some joints that are seismically adequate to be deemed deficient. The economic consequences of such a conservative model can be significant because retrofitting joints is labor-intensive and expensive. The second major shortcoming is that the ASCE-41 guidelines, like the corresponding design rules for joints in

ACI 318-08 (2008), treat joint shear strength as a single, static value that depends on the concrete strength. Mosier (2000) surveyed the research literature on joints with and without transverse reinforcement and found that the shear strength was a function of several parameters, particularly the cyclic loading history, i.e., amplitude, number, and symmetry of loading cycles. Experimental work by Walker (2001) subsequently confirmed this finding for joints without transverse reinforcement.

The research conducted by Mosier and Walker identified several unresolved questions related to joint capacity. The first concerns the relationship between the cyclic joint shear strength and the concrete compressive strength, f'_c. In the United States, most seismic design and evaluation documents for beam-column joints in buildings, e.g., ACI 318-08 (2008), FEMA 356 (2000), and IBC (2003), suggest that the shear strength is related to $\sqrt{f'_c}$, but specifications in other countries (e.g., NZ 3101 2006) are based on other, different relationships. The differences between these various approaches become important when the concrete strength is high. In older buildings, the concrete strength will have increased over time, so an understanding of the effects of process on the joint response is needed (Wood 1992).

A second important issue is that joints tend to degrade gradually, rather than collapsing suddenly, which implies that acceptable joint shear stress and strain limits should be a function of the acceptable damage level. Because damage is a qualitative measure, a relationship is needed between it and quantitative engineering demand parameters (EDPs), such as joint shear stress or strain, if it is to be used for seismic evaluation.

Finally, guidance is needed for the value of the joint shear stiffness to be used in analyses of older frames. Walker (2001) showed that the joint deformations could contribute more than half of the total story drift, in which case frame analyses that use rigid joints are likely to underestimate the story drift. Models that account for degradation in the joint stiffness are therefore needed.

The objectives of the study reported here are to address these three topics using both experimental and analytical means. The experimental research study was developed to study the influence of a wide range of shear stress demand levels in joints without transverse reinforcement. These data were then combined with the research results from Walker (2001) to develop relationships among the critical parameters for use in the seismic evaluation of older frame structures. The results of this research form a basis for evaluating the seismic performance of joints in older reinforced concrete frames. The advances in understanding of joint behavior, the estimates of joint shear stiffness, and the relationships between damage and EDPs provide engineers with evaluation tools that represent a significant improvement over those presently available. The experimental results also provide a basis for development and calibration of analytical models.

TEST PROGRAM

Relatively experimental programs have simulated beam-column joints in older construction that lack transverse reinforcement. Two test programs were carried out to fill this gap in knowledge, and each addressed a different aspect of the problem. Table 1 provides a summary of the two test series, designated as Series 1 and 2 and described in detail by Walker (2001) and Alire (2002), respectively. The naming system for the tests is common to both series, and is as follows. The first four characters define the loading history (described below and shown in Figure 1). Of the four numbers that follow, the first two define the ratio of target joint shear stress to concrete strength, v_j/f'_c, and the last two define the target concrete strength in hundreds of psi. (No decimal points are used.) Thus test PADH-1450 uses the PADH loading history, has a target joint shear stress of $0.14f'_c$, and a target concrete strength of 5000 psi (35 MPa).

The complete set of study parameters consisted of the joint shear stress demand, the displacement history, and the concrete strength. The Series 1 tests were reported by Walker (2001) and were designed to investigate the influence of displacement history on joint response. Seven specimens were tested using four different displacement histories, shown in Figure 1 and indicated in Table 1. The histories included a Symmetric Cyclic Displacement History (SCDH) with monotonically increasing levels of drift, two histories with Constant Drift-ratio amplitudes of 1.5% and 3.0% (CD15 and CD30) and a Pulse-type Asymmetric Displacement History (PADH). The two target joint shear stress demand coefficients $v_j/\sqrt{f'_c}$ were approximately 0.82 and 1.29 (MPa). The lower level corresponds to the FEMA-356 joint shear strength limit, and the upper level represents the ACI 318-08 joint shear strength limit. Therefore the two SCDH specimens from Series 1 served as reference specimens for the Series 2 tests, as indicated in Table 1.

The Series 2 tests were conducted by Alire (2002) and are described in this paper. They were designed to investigate the influences of concrete strength and joint shear stress demand. Mosier (2000) reviewed 15 structures built on the West Coast of the US between 1920 and 1979, and found joint shear stress demands that ranged between $0.19\sqrt{f'_c}$ and $2.18\sqrt{f'_c}$ MPa ($2.3\sqrt{f'_c}$ and $26.3\sqrt{f'_c}$ psi). Very different responses should be expected at the highest and lowest stresses within this wide range. When the joint shear stress is low, the joints will remain relatively undamaged and the majority of the inelastic component of the drift will result from yielding of the beams. This mode of response is ductile, and is the one that contemporary joint designs are intended to achieve. At intermediate joint shear stress values, the beams will yield and the joint will also suffer some damage, while, at high joint shear stresses, the joint may incur significant damage without the beam yielding. The boundaries between these behaviors, expressed in terms of joint shear stress level and other parameters, are at present unclear.

For Series 2, four specimens without joint transverse reinforcement were built with target joint shear stress demands ranging from $0.47\sqrt{f'_c}$ to $2.41\sqrt{f'_c}$ MPa ($5.7\sqrt{f'_c}$ to $29.0\sqrt{f'_c}$ psi), as indicated in Table 1. The Series 2 specimens were designed to complement Specimens SCDH-1450 and SCDH-2250 of Series 1 with respect to the target joint shear stress demand (0850 and 4150) or concrete strength (0995 and 1595), so as to investigate in greater detail the influence of these parameters. (Table 1 shows that, in Specimen SCDH-0850, the measured joint shear stress was significantly higher than the target value. This occurred because the beam bars strain-hardened significantly). The target joint shear stress demands were chosen to investigate the boundaries between the three different behaviors identified above (beam hinging alone, combined beam hinging and inelastic joint deformation, and joint deformation alone).

Older reinforced concrete frames often contain vulnerabilities in addition to the lack of transverse joint reinforcement. The beams may be offset from the columns, the beam or column shear strengths may be insufficient, the bar splices may be inadequate, etc. Because the goal of this study was to investigate joint shear performance, these other failure mechanisms were prevented by using heavy beam and column ties, a column depth of at least 20-bar diameters, continuous beam and column bars, and a column-to-beam flexural strength ratio of approximately 1.4. (In Specimen CDH-4150, bar congestion limited the amount of column steel that could be placed, and consequently the ratio was approximately 1.0). The axial-load ratio was maintained at 0.1 to approximate the average value of 0.12 found in practice by Mosier (2000).

Table 2 and Figure 2 indicate the reinforcement and geometry used for the Series 2 test specimens. The specimens were approximately two-thirds of full scale, where full-scale was defined by a representative building selected by Walker. As indicated in Figure 2, the beams were 400 mm wide by 500 mm deep (16 in. by 20 in.), and the columns were 400 mm wide by 450 mm deep (16 in. by 18 in.) The different target joint shear stress demands were achieved by selecting appropriate beam longitudinal reinforcement. For Specimen SCDH-1595, high-strength beam reinforcement manufactured by MMFX Technologies Corp. was used to maintain the same bond demand ratio as in the other specimens, so the ratio of h_c to d_b exceeded 20 in that specimen.

The SCDH displacement history (Figure 1a), used by Walker on two of his specimens, was used on all four specimens in Series 2 to facilitate comparison with the results of other research. It consisted of 30 symmetric cycles, divided into 10 drift ratio levels of increasing amplitude and included the following drift cycles if the specimen sustained sufficient the residual lateral capacity: 0.1%, 0.25%, 0.5%, 0.75%, 1.0%, 1.5%, 2.0%, 3.0%, 4.0% and 5.0%.

Material Properties

The concrete and steel properties were determined from materials tests and are summarized in Tables 1 and 3. During construction, 150 x 300 mm (6 x 12 in.) concrete cylinders were cast and were cured in sealed molds for 24 hours with the test specimens, then stripped and transferred to a fog room at constant temperature and humidity. The compressive strength was determined on the day of test. The properties of the reinforcing steel were obtained from tension tests. The Raynor (2001) constitutive model was then fitted to the data for purposes of analysis.

Test Set-up and Instrumentation

The test setup and instrumentation used during testing were identical to those of Walker (2001). During testing, the top and bottom of the column were fixed against translation, while equal and opposite vertical displacements were imposed at the beam tips. The beam displacements were measured using linear variable differential transformers (LVDTs) to allow the interstory drift to be calculated. The column shear forces were measured with load cells. Pressure transducers measured the beam shears because of space limitations.

The joint deformations were measured using a purpose-built rig attached to four threaded rods embedded in the core concrete. Taping and oiling the rods prior to casting minimized any confinement that the rod might otherwise have applied to the joint. Two horizontal, two vertical, and two diagonal LVDTs were attached to the rods to create the joint shear rig, as shown in Figure 2. Values of the shear strain were calculated using instruments located with each of the four triangles in the rig and the results were then averaged. Further description of the instrumentation used to monitor all of the sub-assemblage components may be found in Walker (2001) and Alire (2002).

EXPERIMENTAL RESULTS

Qualitative Observations

Both qualitative observations and instrumental measurements were obtained from the experiments. In particular, qualitative observations were made for three subjective damage states, and were then used to develop probabilistic relationships between the level of joint damage and quantitative EDPs such as strain and drift ratio. The damage states recorded were:

1. *Center Joint Cracking* in which diagonal cracks first appeared at the center of the joint,

2. *Initial Spalling* of the joint cover concrete, and

3. *Extreme Spalling*, defined here as exposure of the center column bar.

These damage states represent a subset of those reported by Pagni and Lowes (2006). Figure 3 shows examples of the latter two damage states; Table 4 and Figure 4 show the drift ratios at which they were reached. The drift level reported is the peak drift achieved during the cycle in which the damage state was observed. Because qualitative observations were made only at the cycle peaks, when the loading was temporarily stopped, the recorded drift ratio is an upper bound to the one at which the event occurred.

Center Joint Cracking provided the first observable damage to the joint. The damage occurred between 0.25% and 0.75% drift, with the exception of Specimen SCDH-0850, for which it occurred at 2.0% drift. These relatively low drift levels suggest that, unless the joint shear stress demand is exceptionally low, beam-column joints will experience some cracking, even during moderate earthquakes.

The Initial Spalling damage state occurred between 1.5% and 3.0% drift and, within that range, a higher joint shear stress demand led to spalling at a lower drift ratio. Extreme Spalling occurred between drift ratios of 2.0% and 5.0% and typically occurred at the same time that peak joint shear stress was reached. Both increasing the applied drift ratio and cycling at a constant drift ratio exacerbated the extent of spalling.

The nature of the damage accumulation in the test specimen with low joint shear stress demand (SCDH-0850) differed from that in all of the other test specimens. In Specimen SCDH-0850, joint damage began around the perimeter of the joint in a diamond pattern rather than in the X-pattern that was observed in the other test specimens. Furthermore, joint damage started later in the displacement history, and it was less extensive, than was the case for the other specimens. This result indicates that low joint shear stress demand can limit the joint damage and improve the frame performance.

Measured Data

The measured data were reduced to give the relationship between the cyclic joint shear stress (v_j) and the joint shear strain (γ). That relationship was used, in turn, to evaluate the secant joint shear modulus, G_{sec}, and salient v_j and γ_j values corresponding to the selected damage states for each specimen.

The measured responses are presented both at the sub-assemblage level in the form of column shear force vs. system drift, and at the local level, as average joint shear stress vs. strain relationships. Figure 4 shows the force-drift response curves for specimens SCDH-0850 and SCDH-4150. The measured force-displacements responses indicate that the displacement ductility at maximum lateral load capacity ranged from 9.5 (yield and ultimate drifts of 0.42% and 4.0%) for Specimen SCDH-0850 to 1.2 for Specimen SCDH-4150 (yield and ultimate drifts of 1.75% and 2%). In defining displacement ductility, the yield displacement was defined as the displacement corresponding to initial yield, as measured from the strain gages, and the ultimate displacement was taken as that at which the lateral load reached peak value. Since all specimens were subjected to the same displacement history, the large range of displacement ductility capacities indicates very different contributions of the joint shear deformation to the total drift (Alire 2002). For that reason, joint shear stress and strain provide a better description of the joint behavior than does a global demand parameter such as displacement ductility.

The low level of joint damage and extensive beam yielding in Specimen SCDH-0850 suggest that that specimen lay approximately at the boundary between a joint-shear dominated and beam-hinging dominated response mode. Similarly, the essentially elastic behavior of the beams in Specimen SCDH-4150 suggests that its peak joint shear stress was not controlled by beam bar yielding and therefore that its joint shear strength represents approximately the maximum possible joint shear capacity.

The cyclic joint shear stress-joint shear strain (v_j vs. γ_j) results are shown in Figure 5. Selected damage states discussed earlier are shown on the figures. The results illustrate several important behavioral characteristics, as described below.

1. In all cases, the peak measured joint shear stress achieved was equal to or exceeded the nominal joint shear stress demand, which was calculated from the beam bar forces using a stress of $1.25f_y$. At the end of the test (5% drift), the load was lower than the peak load, so all the specimens may be considered to have reached their lateral drift capacity in the sense that they had lost strength relative to their peak load. <u>This result shows conclusively that joint shear strength is not solely a function of concrete strength</u>. If it were, Specimen SCDH-1595 would have displayed a much higher peak load than Specimen SCDH-4150, because the joints were the same size but made of concretes with nominal strengths of 66 and 35 MPa (9500 and 5000 psi), respectively. In fact, the opposite occurred and Specimen SCDH-4150 carried the higher peak load. It would be reasonable to ask whether this result might have been caused by some other component, such as the beam strength, controlling the peak load and the failure mode. However, this was definitely not the case. In both specimens, the joints suffered extensive damage, of a type that indicated high shear and bond demands, and at the end of the tests the joint shear deformations were responsible for the majority of the drift. By contrast, in the beams and columns, typical signs of failure such as bar buckling and fracture were completely absent.

2. At all levels of joint shear stress demand, the joint shear stress did not drop suddenly but rather remained nearly constant for several levels of applied cyclic drift.
3. A comparison of the cycles at a given drift ratio (indicated on the individual plots in Figure 5) shows that, following initial spalling of the joint, the two specimens with intermediate stress demands (SCDH-0995 and SCDH-1595) showed a marked increase in joint shear strain, even though the drift remained constant for two more cycles. This behavior may be explained by the change in the relative stiffness values of the beam and joint and the susceptibility of the joint to damage. In Specimen SCDH-0850, the joint suffered relatively little degradation, so its stiffness remained nearly constant throughout the three cycles of each set, and the apportionment of drift between beam flexural deformations and joint shear deformations remained relatively constant as well. In Specimens SCDH-0995 and SCDH-1595, the higher joint shear stress led to cyclic degradation of the joint, so its secant stiffness dropped, whereas that of the beam stayed relatively constant. Thus, during the second and third cycles of the set, a larger proportion of the total drift was caused by joint deformation and the joint shear strain consequently increased. In Specimen SCDH-4150 the joint shear stress was so high that joint deformations accounted for a large portion of the drift, even in the first cycle, so they changed little during the second and third cycles of the set for most of the drift cycles.

These observations show the need for a basis for quantifying joint performance that reflects the observed behavior better than does a model solely based on joint shear, e.g. the FEMA 356 model. Figure 6 shows the relationship among drift ratio, normalized joint shear stress (defined as $v_j/\sqrt{f'_c}$) and damage states, for all the SCDH specimens. Each curve corresponds to a single damage state. (For states in which specimens SCDH-0995 and SCDH-1595 overlie one another, only five (5) points appear.)

The curves are separated vertically and slope down to the right, implying that damage is a function of both joint shear stress demand and drift. The slopes are relatively small, which suggests that drift ratio is the more important variable. However, joint shear stress also plays a role. This may be illustrated by considering the damage corresponding to 2% drift. For low applied stress, the joint suffers little damage. For example, at this drift level Specimen SCDH-0850 had just experienced Center Joint Cracking. If a higher drift level, say 3%, were used, the peak permissible shear stress needed to limit the damage to Center Joint Cracking could be obtained by back-projecting the curve. Unfortunately the first cracking curve is extremely non-linear, so such back-projection is not quantitatively robust, but the joint shear stress would clearly have to be less than the $0.47\sqrt{f'_c}$ (MPa target), or $0.71\sqrt{f'c}$ (MPa measured), experienced by Specimen SCDH-0850. At the other extreme, the highly stressed Specimen SCDH-4150 sustained significant joint damage (Extreme Spalling) at 2% drift ratio. In that specimen, the beam bars yielded just as the peak load was reached. This suggests that the specimen could not have carried a joint shear stress much higher than the target value, $2.4\sqrt{f'_c}$ (MPa), or measured value, $2.1\sqrt{f'_c}$. These two specimens thus define approximately the limits of the two independent damage modes: beam hinging and joint shear. Confirmation of this finding, by means of further experiments with different joint shear stress demands and concrete strengths, is desirable.

Figure 6 also shows the limits specified in FEMA-356 (2001) and ACI-318-08 (2008), which express the joint design in terms of joint shear stress alone. In design, the story drift ratio is usually limited to approximately 2%, and this value can be used to illustrate the suitability of the FEMA and ACI limits. If the design is intended to avoid joint damage altogether, Figure 6 shows that even the FEMA joint shear stress limit of $0.83\sqrt{f'_c}$ MPa ($10\sqrt{f'_c}$ psi) is too liberal, because the joint will suffer Center Joint Cracking before the 2% drift is reached. However, if Extreme Spalling is considered acceptable, then even the ACI limit is much too restrictive, because the joint shear stress limit could be increased to approximately $2.1\sqrt{f'_c}$ (MPa) before the damage exceeded the permissible state. This latter situation might result in joints being retrofitted unnecessarily.

These results indicate that the seismic performance evaluation of joints in existing reinforced concrete frames cannot be based on a single level of joint shear stress. A relationship is needed between the demands, including both frame deformation and joint shear stress, and the acceptable damage state.

Development of a universal relationship for all joints is not straightforward. Evaluation of the joint performance in the intermediate range of the joint shear stress is not a simple matter, as indicated in Figure 6. The specimens within the joint shear stress ratio range of 0.7 to $1.3\sqrt{f'_c}$ (MPa) do not show a strong trend with regard to the normalized joint shear stress demand. However, this is the range in which most joints will lie. Further difficulties are caused by the fact that the strength degrades with cycling, and that the extent of bar yielding (with its implications for degradation of bond strength) may also be important.

To illustrate this, consider the normalized joint shear stress–drift response envelopes shown in Figure 7. The envelopes for specimens SCDH-0995 and SCDH-1450 were almost identical, even though Specimen SCDH-0995 suffered more joint damage than did Specimen SCDH-1450 at the same drift ratio. This difference may be due to the smaller bond stress demand in Specimen SCDH-0995, which in turn may have resulted in a lower bar-slip component at a similar joint shear strain. Thus, evaluation of the joint performance may require consideration of parameters in addition to joint shear stress demand, including the cyclic drift and/or joint shear strain history and the bond demand on the beam bars.

CUMULATIVE PROBABILITY CURVES FOR DAMAGE EVALUATION

The test results indicate that there is a link between the level of joint shear stress, accumulated joint deformation, and the specified level of damage. Therefore, to achieve the goals of performance-based seismic engineering, relationships between these demand parameters and damage must be developed. In the interest of obtaining approximate relationships now, simple statistical relationships between damage levels and EDPs such as joint shear strain and drift were developed using the combined experimental results. Approximate joint stiffness values for use in analyses of frames are discussed in the following section. A complete description of such a relationship requires an extensive modeling effort, and may also require additional testing.

To quantify performance, relationships between damage and EDPs, using Cumulative Probability Curves (CPC), were derived. The damage states of Center Joint Cracking, Initial Spalling, and Extreme Spalling were related to several EDPs. Since engineers often use global demand parameters such as interstory drift ratio and displacement ductility (e.g., FEMA 356), these EDPs were considered. However, the previous analysis of the data suggests that joint shear stress and strain are more appropriate variables with which to evaluate joint damage. Therefore, these parameters were also used to develop CPCs.

The mean and coefficient of variation (COV) of the data were used to determine the most appropriate parameter. For each EDP, mean and COV values are provided in Table 5. In Figures 8 through, 10, only CPCs for the best demand parameter are presented for each damage state. Curves for the other parameters may be found in Alire (2002).

For Center Joint Cracking, much the lowest COV (29%) was provided by the normalized joint shear stress demand at cracking, which suggests that Center Joint Cracking is more closely correlated with joint shear stress than with any other parameter. For the specimens tested, the mean joint shear stress at cracking was 86% of the $0.625\sqrt{f'_c}$ (MPa) that ACI318-08 defines as f_r, the modulus of rupture. Table 5 shows that a slightly better correlation still was obtained by normalizing v_j with respect to $\sqrt{f'_c}$ rather than f_r. Figure 8 shows the Cumulative Probability Curve for the Center Joint Cracking as a function of normalized joint shear stress.

The other two damage states considered, Initial Spalling and Extreme Spalling, are defined by the extent of damage to the joint. Joints with Initial Spalling damage state are generally repairable. CPC relations were developed for drift ratio, displacement ductility, and joint shear strain for these two damage states. For Initial Spalling, the smallest COV (34%) was found using the local EDP of joint shear strain. On average, this damage state occurred at a joint shear strain of 0.011 rad. Figure 9 shows the relationship between Initial Spalling and joint shear strain.

Extreme Spalling represents a damage state at which the joint would need to be replaced. All of the test specimens eventually exhibited damage patterns that could be categorized as Extreme Spalling. Extreme Spalling was correlated with drift, displacement ductility, and joint shear strain. Analysis of the data shows that, if all the specimens are used, the Extreme Spalling CPCs are most closely correlated to drift, because it leads to the smallest COV. However, if only the SCDH specimens are considered, joint shear strain proves to be the better indicator. Joint shear strain is the recommended parameter because use of specimens subjected to the same drift history (i.e. SCDH) minimizes the effects of the demand history, which have already been shown to influence the response (Walker 2001). Figure 10 illustrates the difference.

The foregoing discussion showed that local demand parameters, such as joint shear stress and strain, provide better estimates of local damage than do global parameters, such as drift. This conclusion is based largely on the COV of the measured values of the different EDPs at the damage state of interest. It is also consistent with the fact that the global parameters include components of unrelated response components, (e.g. story drift includes a component due to beam bending), and so should be expected to correlate less well.

EVALUATION OF JOINT SHEAR STIFFNESS

In none of the eleven joints did the joint become unable to carry the column axial load, nor did the lateral stiffness drop to zero. In that formal sense, no joint collapsed. Thus, to gain insight into potential failure of a frame, other definitions of failure must be investigated. Excessive loss of stiffness is the most obvious candidate, because it leads to structural failure through instability or to functional failure through excessive drift. (The test set-up precluded instability, because the column was held stationary and the load remained vertical). The joint stiffness influences both behaviors, so its value is of interest. In addition, the frame performance depends on the damage sustained by the other frame components (Pagni and Lowes 2004). The results from Walker (2001) and Alire (2002) demonstrated that an increase in either the joint shear stress demand or the damage state results in an increase in the contribution of the joint deformation to the drift. Therefore, evaluation of the seismic performance of existing frames requires relationships among the joint stiffness, the shear stress demand and the damage state.

The joint stiffness degrades with cycling in a complicated manner and was the subject of a separate enquiry (Anderson et al., 2008). However, to facilitate immediate implementation in existing professional structural analysis software, a simple model intended to capture the major trends of the response was developed. For each of the eleven specimens tested, the secant stiffness of the joint was computed at critical stages of the load history. These were: First Cracking at the center of the joint, First Yield in the beam bars, and Initial Spalling of the joint. In each case, the stiffness is expressed as a shear modulus ratio G_{sec}/G_{el}, where G_{sec} and G_{el} are respectively the instantaneous secant and the (uncracked) elastic shear moduli of the joint. The secant stiffness was computed from the joint shear stress and strain and was evaluated only at the first peak to a new drift level. Joint shear stress-strain envelope curves, defined by these points, are shown in Figure 11. Estimates of G_{sec} at different strain levels can be obtained from that figure. In the following discussion, only the values for the SCDH specimens are used in order to avoid the influence of loading histories.

The modulus ratio G_{sec}/G_{el} was computed for each of the SCDH specimens, including those from Series 1, and its mean and coefficient of variation were obtained for each damage state. Specimen SCDH-0850 was excluded from the statistics because its behavior differed significantly from that of the others. At first cracking, G_{sec}/G_{el} had a mean and COV of 0.32 and 42%, respectively. At Initial Spalling it had a mean and COV of 0.055 and 30% respectively.

At First Yield (Yielding damage state), the stiffness ratio G_{sec}/G_{el} was found to vary with the joint shear stress demand, which in turn is a function of the flexural steel ratio of the beams. An equation was developed to relate G_{sec}/G_{el} at first yield to the nominal joint shear stress. Its form was first obtained from the fact that the drift at first yield was found to be approximately linearly related to the joint shear stress. However, it can be shown (Alire 2002) that the contribution to the drift of beam curvature at first yield is a function of the beam depth and the yield strain of the bars, but is almost independent of the beam strength. By assuming this, and that the column contribution to drift was 2/3 of its yield value (since $M_{n,col}/M_{n.beam}$ was designed to be approximately 1.5), and by assigning the remaining deformation to joint shear, an equation for the joint secant shear modulus of the form

$$\frac{G_{sec}}{G_{el}} = \frac{c_1}{\left(1 - c_2/v_j\right)} \leq 0.32 \qquad (1)$$

was derived. Fitting this equation to the measured joint shear stress and strain data led to best fit values of $c_1 = 0.039$ and $c_2 = 3.5$ MPa.

The shear modulus ratios (for all specimens, including those tested by Walker (2001)) are plotted against the joint shear stress, v_j, in Figure 12. This approach is necessarily approximate. However, in the short-term absence of a better joint model, it provides practicing engineers with an approximate way of including joint deformations in frame analyses. The fact that the joint deformations represent a significant fraction of the total drift shows that approximating it is an improvement over ignoring it. The importance of joint flexibility is indicated by the fact that, even prior to visible cracking, the joint shear stiffness is only 32% of its gross value.

SUMMARY AND CONCLUSIONS

A program of experiments was conducted on reinforced concrete beam-column joints without transverse reinforcement. From qualitative observations and analyses of the measured data, probabilistic relationships were developed that correlated EDPs to pre-defined damage states. Approximate values of the effective joint secant shear modulus were developed for joints with a range of joint shear stress demands at three different levels of damage. The joint stiffnesses derivable from these shear moduli are suitable for immediate use in frame analyses of older buildings with joints without transverse reinforcement.

The experimental results led to the following conclusions:

1. The beam-column joints tested were subjected to nominal joint shear stresses that varied from $0.47\sqrt{f'_c}$ to $2.41\sqrt{f'_c}$ MPa. In all cases the joint incurred serious damage.
2. Larger shear stress demands lead to more severe damage and faster damage accumulation.
3. Joint shear stress capacity is not a function of concrete compressive strength alone, as current seismic design and evaluation provisions suggest. The other parameters found to influence the peak joint shear stress include: cyclic loading history, joint shear stress demand, extent of beam bar yielding, and bond capacity.
4. Specimen SCDH-0850 was designed and tested with the intention of determining a joint shear stress demand below which no joint damage would occur, thereby forcing all of the nonlinear behavior into the plastic hinges at the ends of the beams. If such a threshold joint shear stress exists, it lies below the nominal shear stress demand of $0.47\sqrt{f'_c}$ MPa experienced by this specimen. However, it is likely to lie close to this limit, because joint damage in Specimen SCDH-0850 was much delayed in comparison with that in other specimens.
5. The nominal joint shear stress of $2.41\sqrt{f'_c}$ MPa sustained by Specimen SCDH-4150 is believed to be close to the maximum achievable value under any loading. In most specimens significant joint damage started only when the beam bars yielded, but in Specimen SCDH-4150 the beam bars only just yielded at the end of the test, by which time significant joint damage had already occurred.
6. First cracking of the joint correlated most closely with joint shear stress, and on average, occurred at a joint shear stress of $0.86f_r$.

7. Damage states associated with different levels of spalling were reached after different numbers of cycles but they correlated most closely with joint shear strain. For a given deformation history, higher joint shear stresses caused the damage states to be reached earlier. Initial Spalling occurred at a mean joint shear strain of 0.011 rad. The joint shear strain at Extreme Spalling varied among specimens from 0.022 to 0.040 rad. with a mean of 0.035 rad. for all specimens and 0.026 rad. for specimens subjected to the same drift history. These strains corresponded to drift ratios in the range 2% to 5%.
8. The joint shear deformation and the beam bar pullout both contribute significantly to the total drift. Frame analyses that treat the joint as rigid, as is commonly done in practice, will under-estimate the true drift for a given load and will not provide a reliable estimate of the frame performance.
9. Values for the secant joint stiffness were derived as fractions of the elastic shear modulus, G_{el}, for different damage states. In the absence of a more sophisticated model, they are suitable for inclusion in frame analyses to approximate the true flexibility of the system. Mean shear modulus values of $0.32G_{el}$ at first cracking and $0.055\ G_{el}$ at initial spalling were found. At first yield, the secant stiffness varied with joint shear stress demand and an equation was developed to relate G_{sec}/G_{el} to v_j.

ACKNOWLEDGEMENTS

Funding for the experimental testing was provided by NSF under Award Number EEC-9701568 through the PEER center. The Department of Civil and Environmental Engineering at the University of Washington (UW) supported the graduate studies of the first author. Meredith Anderson and Brad Johnson, UW graduate and undergraduate students, respectively, helped with the experimental program; their efforts are gratefully acknowledged. The authors would also like to thank the UW laboratory staff, Vince Chaijaroen and Kenny Knowlan, PEER REU Susan Smelnek and Student Assistant V.J. Chaijaroen for their assistance.

REFERENCES

ACI Committee 318 (2008). “Building Code Requirements for Structural Concrete (ACI 318-08) and Commentary (ACI 318R-08): An ACI Standard,” American Concrete Institute, Farmington Hills, MI.., 2008

ASCE (2007) “Seismic Rehabilitation of Existing Buildings, ASCE/SEI 41-06”, American Society of Civil Engineers, 416 p.

Alire, D.A. (2002). "Seismic Evaluation of Existing Unconfined Reinforced Concrete Beam-Column Joints", MSCE thesis, University of Washington, Seattle, 250 p.

Anderson, M.R., Lehman, D.E. and Stanton, J.F. (2008). “A Cyclic Shear Stress-Strain Model for Joints in Older Reinforced Concrete Frames”. Engineering Structures, vol 30, No. 4, April 2008, pp. 941 – 954.

FEMA Publication 356 (2000). “Prestandard and Commentary for the Seismic Rehabilitation of Buildings”, Building Seismic Safety Council, Washington, D.C., November.

IBC (2003) International Building Code International Conference of Building Officials, Whittier, California, U.S.A., 2003

Meinheit, D. and Jirsa, J. (1977) Shear Strength of JointsAustin : Dept. of Civil Engineering, Structures Research Laboratory, the University of Texas at Austin, 1977

Mosier, G. (2000). “Seismic Assessment of Reinforced Concrete Beam-Column Joints”. MSCE thesis, University of Washington, Seattle. 218 p.

NEES-GC (2009) http://peer.berkeley.edu/grandchallenge/index.html

NZS 3101:06 (2006) New Zealand Concrete Standard Part 1-The Design of Concrete Structures, 1995

Pagni, C. A., and Lowes, L. N. (2006). "Fragility Functions for Older Reinforced Concrete Beam-Column Joints." Earthquake Spectra, Vol. 22, No. 1, pp. 215-238.

Raynor, D.J. (2001). **"**Bond Assessment of Hybrid Frame Continuity Reinforcement**".** MSCE thesis, University of Washington, Seattle. 248 p.

Walker, S.G. (2001). "Seismic Performance of Existing Reinforced Concrete Beam-Column Joints". MSCE Thesis, University of Washington, Seattle. 308 p.

Wood, S. (1992). "Evaluation of the Long-Term Properties of Concrete", Research and Development Bulletin RD102, Portland Cement Association, 1992, 99 pages.

NOTATION LIST

d_b = bar diameter

f'_c = specified concrete strength

f_r = modulus of rupture of concrete

G_{el} = elastic shear modulus of uncracked concrete

G_{sec} = secant shear modulus of concrete

h_c = column depth

v_j = joint shear stress

γ_j = joint shear strain

Figure 1

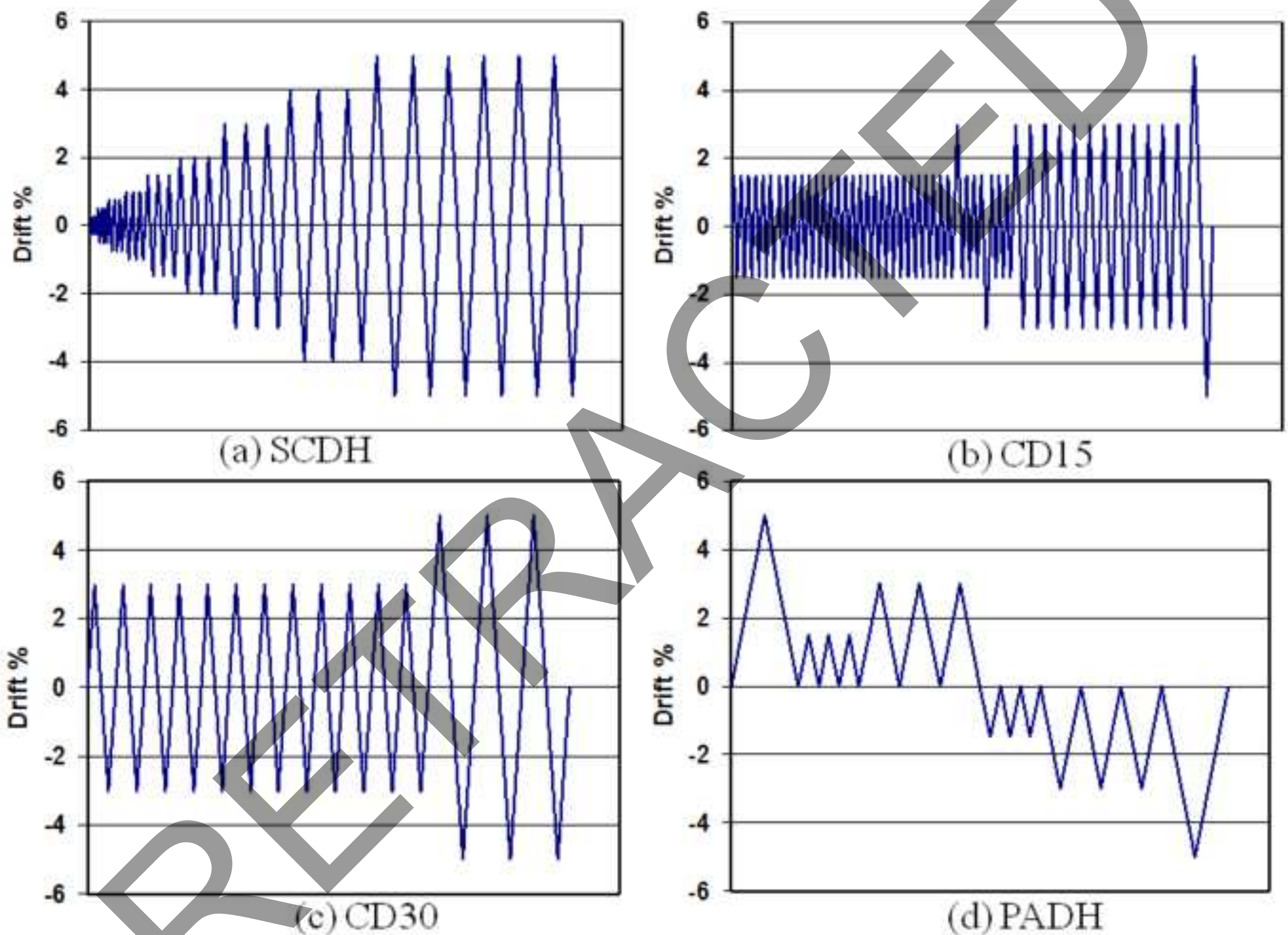

Figure 2

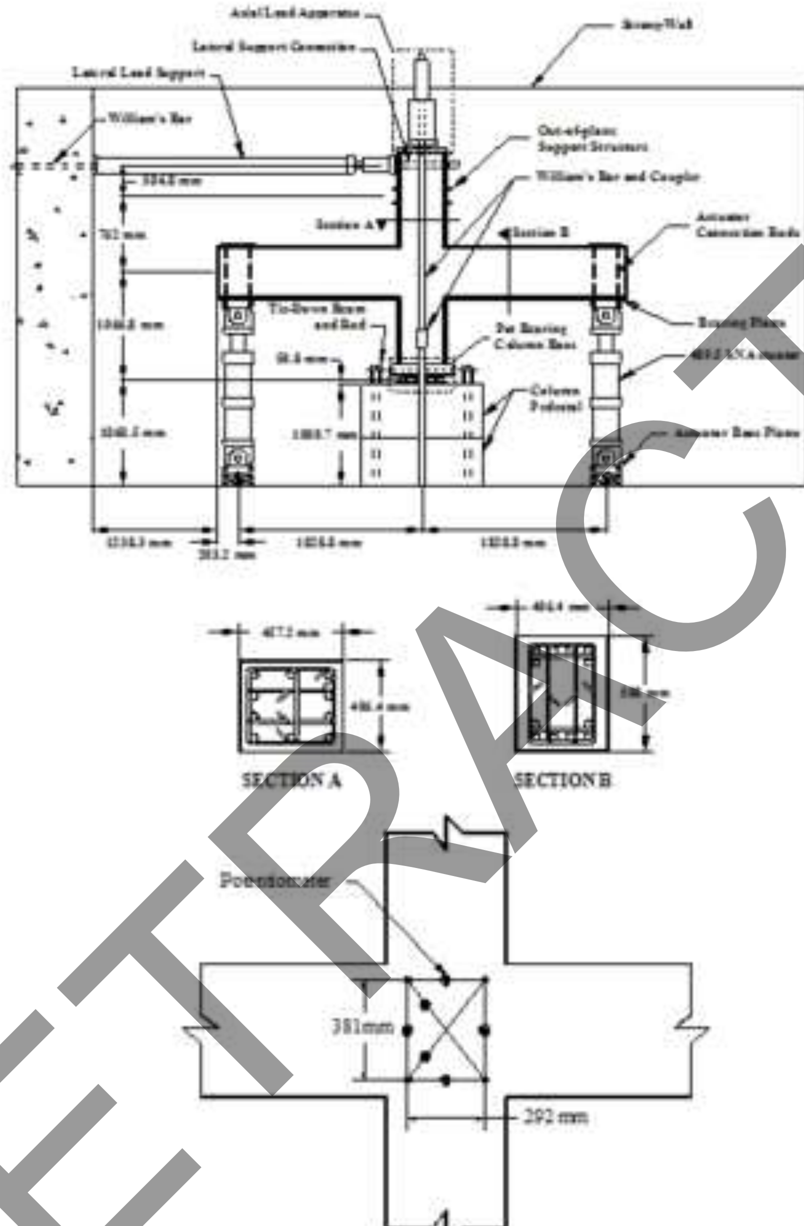

Figure 3

(a) Initial spalling (b) Extreme spalling

Figure 4

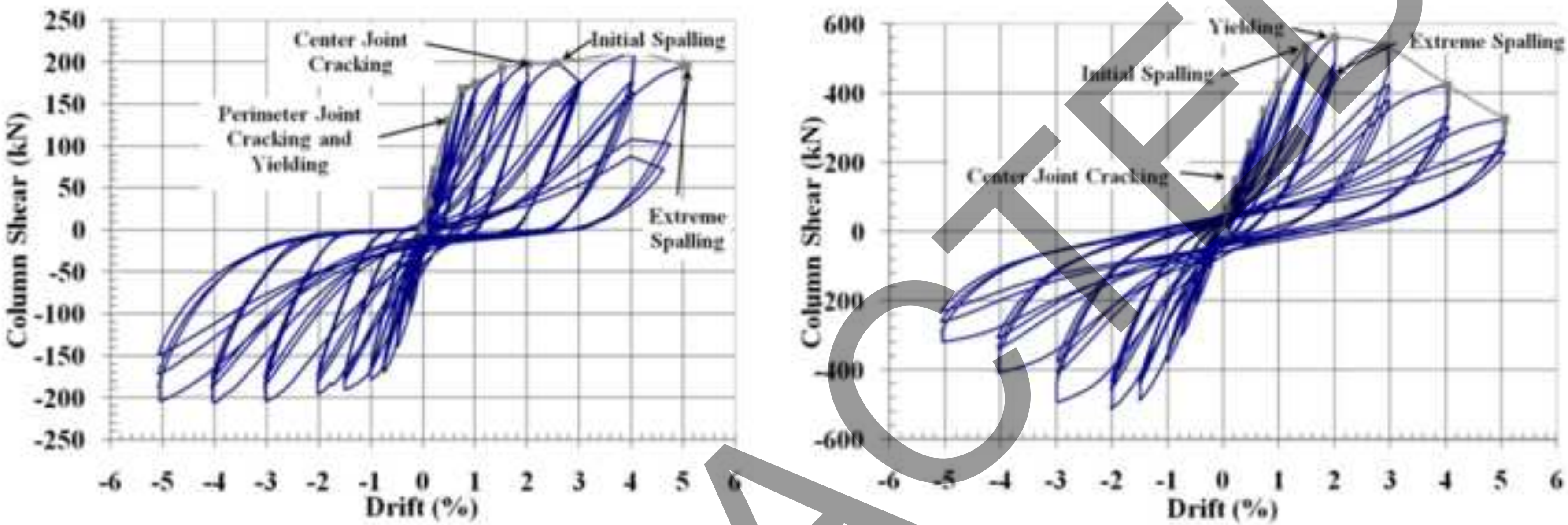

(a) SCDH-0850

(b) SCDH-4150

Figure 5

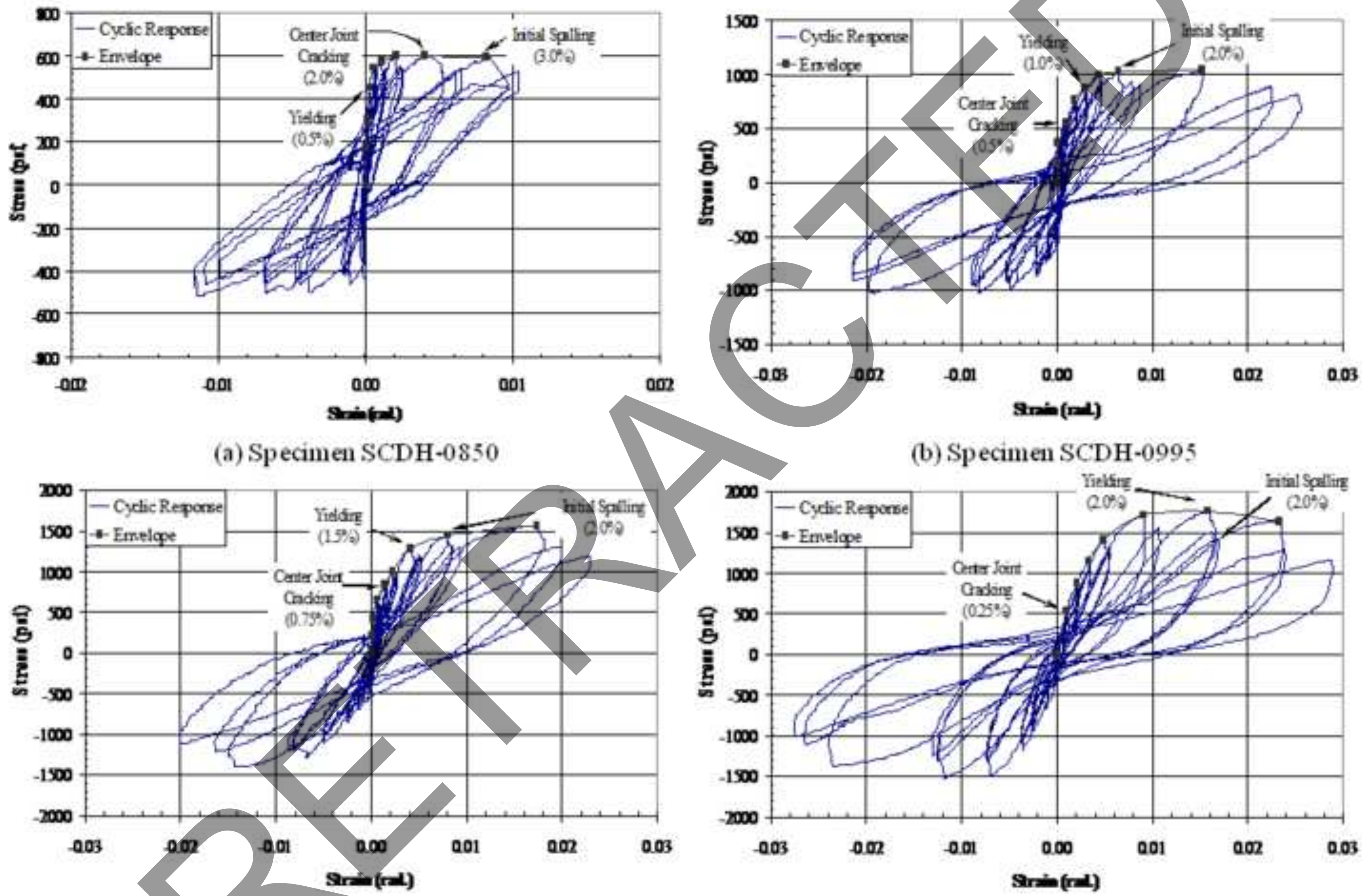

(a) Specimen SCDH-0850

(b) Specimen SCDH-0995

(c) Specimen SCDH-1595

(d) Specimen SCDH-4150

Figure 6

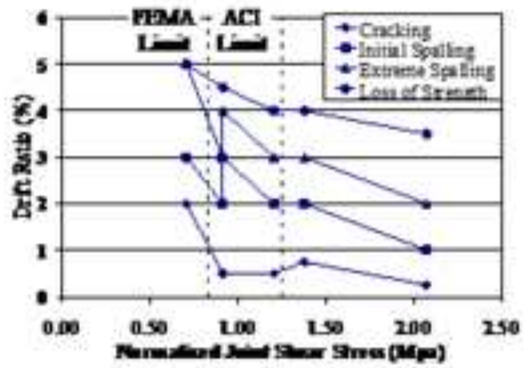
FEMA Limit
ACI Limit
Cracking
Initial Spalling
Extreme Spalling
Loss of Strength
Drift Ratio (%)
0
1
2
3
4
5
6
0.00
0.50
1.00
1.50
2.00
2.50
Normalized Joint Shear Stress (Mpa)

Figure 7

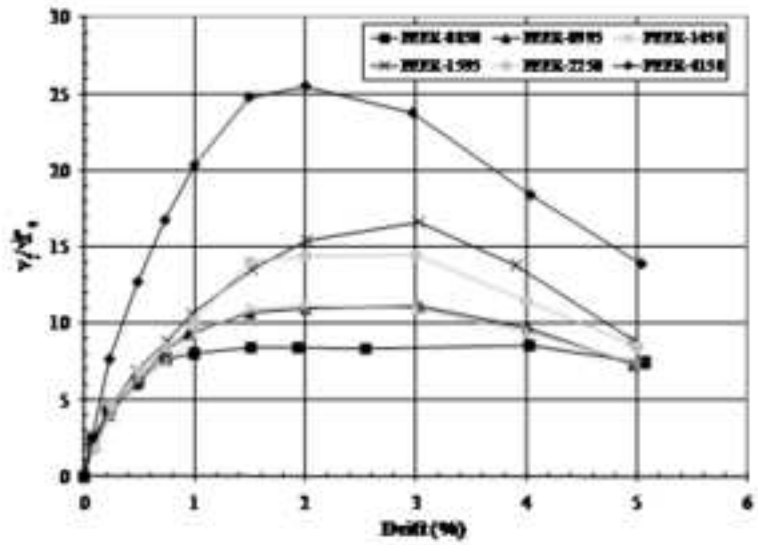

Figure 8

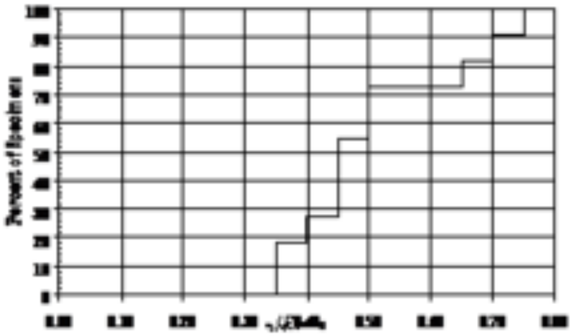

Figure 9

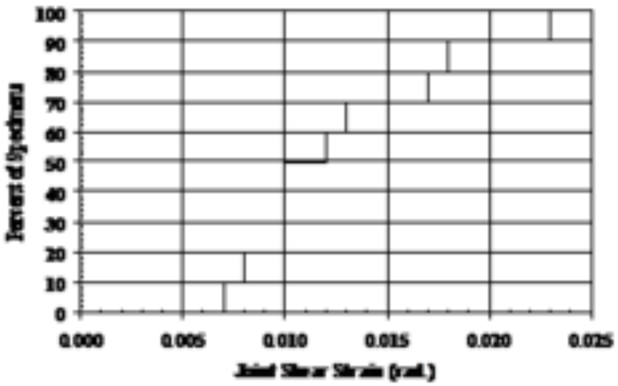
100
90
80
70
60
50
40
30
20
10
0
0.000
0.005
0.010
0.015
0.020
0.025
Joint Shear Strain (rad.)

Figure 10

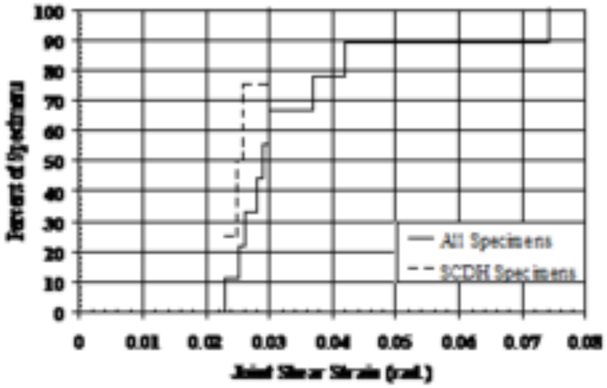

100
90
80
70
60
50
40
30
20
10
0
Percent of Specimens
0
0.01
0.02
0.03
0.04
0.05
0.06
0.07
0.08
Joint Shear Strain (rad.)
All Specimens
SCDH Specimens

Figure 11

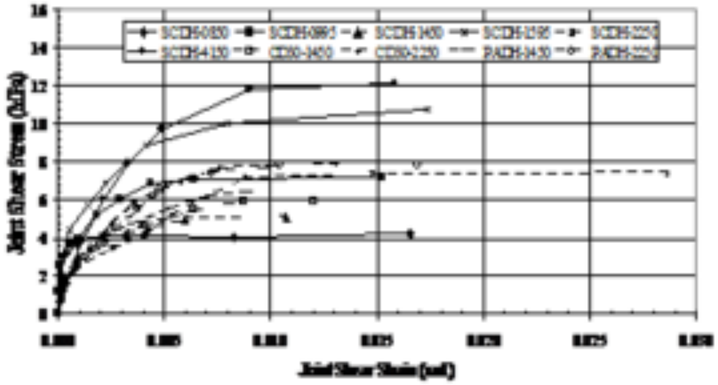

Figure 12

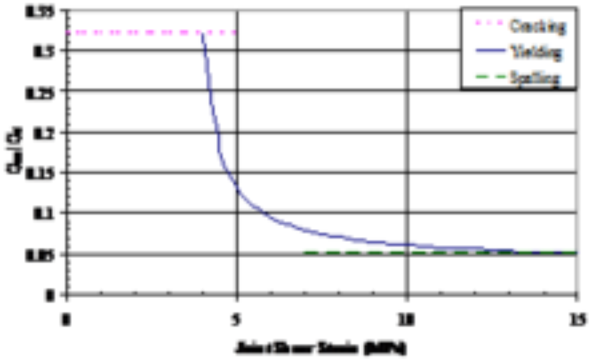

Figure Titles Alire et al.

Figure 1. Displacement Histories

Figure 2. Test Setup, Specimen Geometry, and Joint Instrumentation

Figure 3. Illustration of (a) Initial Spalling, (b) Extensive Spalling

Figure 4. Force-drift response curves

Figure 5. Joint shear stress-joint shear strain responses for Series 2 specimens

Figure 6. Relationship among drift ratio, measured joint shear stress, and damage states for SCDH specimens

Figure 7. Normalized joint shear stress vs. drift ratio envelopes

Figure 8. CPC for normalized joint shear stress at Center Joint Cracking.

Figure 9. CPC for Joint shear strain at Initial Spalling

Figure 10. CPC for Joint shear strain at Extreme Spalling

Figure 11. Joint shear stress-strain envelopes

Figure 12. Joint shear modulus ratio